Proceedings of 14th IOE Graduate Conference
Peer Reviewed
Year: 2023 Month: December Volume: 14
ISSN: 2350-8914 (Online), 2350-8906 (Print)

Harmonic Analysis of a Simply Supported Trash Rack Bar in Hydropower Intakes with Varying Cross-sections and Uniformly Distributed Harmonic Force

Sunil Maharjan [a], Raj Kumar Chaulagain [b], Mahesh Chandra Luintel [c]

[a,b] *Department of Automobile and Mechanical Engineering, Thapathali Campus, IOE, Tribhuvan University, Nepal*
[c] *Department of Mechanical and Aerospace Engineering, Pulchowk Campus, IOE, Tribhuvan University, Nepal*
[a] sunil.mhrjn22@gmail.com, [b] rajkrc12@gmail.com, [c] mcluintel@ioe.edu.np

Abstract
In hydropower intakes, a simply supported trash rack is used to prevent trash from entering the water conveyance system. Due to variable load requirements in the turbine, the trash rack experiences vibration during power plant operation. The resonance causes fatigue damage to the trash rack bar and is not limited to the trash rack itself. It is directly linked to the hydro turbine. Any damage due to trash in the turbine may cause the plant to shut down, powerhouse damage, life loss, results in revenue loss among many. Thus, the study of the vibration of a trash rack is important and this paper investigates trash rack bars of varying cross-sections and uniformly distributed harmonic force which may help hydropower designers avoid catastrophic failure in power plants. The equation of motion for the transverse vibration of the rectangular bar was derived and solved for the free and forced vibration. For the first mode shape of transverse vibration, the percentage error of free vibration analysis between analytical and numerical methods was found to be under 10 %, while for higher mode shapes, it was found to be 33 %. For the harmonic analysis, the Mode Superposition Principle (MSUP) was used. Plotting the equivalent stress and amplitude against the harmonic force reveals a linear relationship. To verify the structural integrity of the bar at resonance, the equivalent stresses were then compared to the permissible stresses.

Keywords
Transverse Vibration, Modal and Harmonic Analysis, Trash Rack Bar, Simply Supported, Amplitude, Equivalent Stress

1. Introduction

To prevent trash from getting into the water conveyance system, virtually all hydropower plants have a trash rack at the entry. The trash rack bar is designed as a simply supported beam because it offers easy installation and maintenance, simple design, cost-effectiveness, replacement and repair if damaged, ability to withstand variable water pressure and most importantly it has a predictable behaviour under load which ensures the safety of both personnel and structure. Size and shape are determined by the specifications of the project. They are made from bars, which are often rectangular sections that are angled or vertically orientated at the necessary spacing. These bars link together to create a panel vertically or horizontally covering the orifice at intakes.

An unavoidable consequence of protection against trash via a rack is vibration. Vibration causes damage to the structure, reduces its effectiveness in trapping debris, and increases maintenance costs, cracks and fatigue damage. Research has shown that trash rack vibration is caused by a combination of factors, including the flow of water through the rack, the shape and geometry of the rack, and the properties of debris that are trapped in the rack.

The most common method to reduce trash rack vibration is by optimizing the design of the rack. And, there are no widely accepted guidelines for the design and maintenance of trash racks to prevent vibration. Therefore, an effect of vibration on individual bars of different cross-sections is presented.

Among an object's distinguishing properties is vibration. The initial displacement is transient, and the type of deformation is contingent upon the boundary condition referred to as the system's free vibration. The object comes to rest as a result of the damping force produced inside the system after a certain amount of time. In free vibration, mode forms corresponding to the natural frequencies are obtained. Force, pressure, temperature, wind, and other factors can all cause the system to vibrate forcefully and may cause resonance. Resonance occurs when the system's frequency coincides with its natural frequency. The system oscillates at its highest amplitude when in resonance, which might lead to system fatigue failure.

A formula for determining the natural frequency, the vortex shedding frequency, and the suggested ratio between them was put out by Levin. It was also pointed out that a bar's inherent frequency in water can differ significantly from that of the bar in air[1]. Sell presented the detailed design of a trash rack for hydropower[2]. Naudascher in his publication explicitly covered the flow-induced vibration (FIV)[3]. IS 11388 which is the basis of this paper relies upon Levin and Sell[4]. Nascimento found out that the added mass effect due to water reduces the natural frequency by about 30 per cent which as per Levin is verified. Further, it was noted that the damage to the trash racks is due to several operating conditions resulting in fluid-dynamic exciting forces acting at resonant frequencies [5]. Crandall et al. while experimenting on the half-scale model discovered "locked-in" during normal flow rates. They changed the bar cross-section and added damping to eliminate this phenomenon[6]. Nguyen and Naudascher determined the effect of Karman vortices and impinging leading-edge vortices at zero flow incidence for

different rectangular sections[7]. A natural frequency that is twice the vortex shedding frequency is what Hollenstein discovered to prevent vibration from producing maximum amplitude[8]. Huang et al. compared experimental and numerical results for natural frequencies and found a maximum error of -1.4% to 6.7% without affecting mode shape both in air and water. It is also found that the water decreases the natural frequency and the added mass depends on mode shapes[9]. According to Haddara and Cao's findings, the additional mass brought by water during submergence is dependent on the depth of submergence up until a certain point, after that the added mass becomes constant. Through experiments, it was discovered that the depth of submergence had no effect on the mode shapes and that damping greatly rises after the plate comes into contact with water and stays that way even after varying depths of submergence[10]. Using a solid-acoustic finite element model that represents sound as a fluid, Stenius et al. investigated fluid-structure interaction (FSI) and reported that deviation in natural frequency air can be reduced by 70% from simple to complicated geometries[11]. Gawali et al. carried out the modal analysis of a simply supported beam with/without crack both analytically and experimentally. They found out that frequencies of cracked beams decrease with increasing crack depth due to reduced stiffness[12]. Kumar et al.. studied modal analysis of cantilever, simply supported and fixed beams and found that deviation from analytical to numerical and experimental was found to be within 6% and 19.31% respectively[13]. Ghodge et al. carried out the modal analysis of the cantilever and simply supported the beam using structural steel, aluminium alloy, copper alloy, and grey cast iron with added mass and found that structural steel with higher natural frequency[14]. Xue et al.. used a reduced-order model in a large trash rack to study the dynamic nature and verified vibration in the trash rack occurs due to the non-linear vibro-impact aspect which can be helpful in optimizing structural vulnerability during an early stage[15].

The researchers presented formulae to determine the natural frequency, studied flow-induced vibration and their relationship with resonance, experimented with the half-scale model, presented results using computational fluid dynamics, and developed models such as solid acoustic finite element and reduced order to study vibration. However, research based on trash rack bars in hydropower intakes with varying cross-sections and uniformly distributed harmonic force was found scarce which this paper aims to fulfil. Furthermore, apart from the modal analysis, a different approach to harmonic analysis in terms of the stress and deflection of the bar during resonance was studied and presented in this paper.

2. Methodology

The expression for the kinetic and potential energy was formulated and the Lagrange principle was used. The work done by the external longitudinal force was then formulated. And, the extended Hamilton's principle was applied to combine the energies of the system and the equation of motion for the transverse vibration was derived. The equation of motion was solved for

- free vibration: simply supported boundary condition, and
- forced vibration: simply supported boundary condition with external harmonic force.

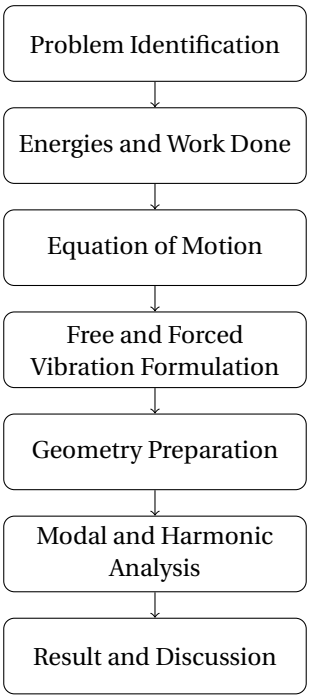

Figure 1: Methodology

The bar's natural frequencies were determined using the modal equation derived from the free vibration, and the numerical result was compared with the results. Furthermore, the clear spacing and head difference in bars were used to compute the necessary harmonic force. Next, the Strouhal number, effective velocity, and bar thickness were used to calculate the forcing frequency. For harmonic analysis, the mode superposition principle (MSUP) was used. The phase angle, maximum amplitude, and resonance frequency were obtained from the harmonic study. Then, the resonance frequency and phase angle obtained from the frequency response were used to obtain the maximum equivalent stress and compared with permissible stress to verify the stability of the bar during resonance.

3. Mathematical Derivation

3.1 Equation of Motion of a Bar

Considering a simply supported rectangular bar of length L with a uniformly distributed load $f(x,t)$ with beam density ρ, modulus of elasticity E, cross-sectional area A, and moment of inertia I. Then, the transverse displacement of the bar is given by $w(x,t)$. Then, the kinetic energy of the rectangular bar can be expressed as [16]

$$T = \frac{1}{2}\int_0^L \rho A\left(\frac{\partial w}{\partial t}\right)^2 dx \tag{1}$$

The strain energy of the rectangular bar can be expressed as [16]

$$V = \frac{1}{2}\int_0^L EI_y\left(\frac{\partial^2 w}{\partial x^2}\right)^2 dx \tag{2}$$

The Lagrangian functional for the system can be expressed as [16]

$$L = T - V = \frac{1}{2}\int_0^L \rho A\left(\frac{\partial w}{\partial t}\right)^2 dx - \frac{1}{2}\int_0^L EI_y\left(\frac{\partial^2 w}{\partial x^2}\right)^2 dx \quad (3)$$

The work done by the external force can be expressed as [16]

$$W_{nc} = \int_0^L f \cdot u\, dx \quad (4)$$

The extended Hamilton's principle can be expressed as [16]

$$\int_{t_1}^{t_2} (\delta L + \delta W_{nc})\, dt = 0 \quad (5)$$

and, the equation of motion for the assumed system can be derived from equation (5) as [16]

$$\rho A\frac{d^2 w(x,t)}{dt^2} + EI\frac{d^4 w(x,t)}{dx^4} = f(x,t) \quad (6)$$

3.1.1 Free Response: Transverse Vibration

Substituting $f(x,t) = 0$ in equation (6) and for a simply supported bar with boundary conditions as $w(0,t) = 0; w"(0,t) = 0$ and $w(L,t) = 0; w"(L,t) = 0$, the natural frequency can be determined as [16]

$$\omega_n = \left(\frac{n\pi}{L}\right)^2 \sqrt{\frac{EI}{\rho A}} \quad ; \quad n = 1,2,3,... \quad (7)$$

The general steady-state response of the beam undergoing transverse vibration is given by [16]

$$w(x,t) = \sum_{i=1}^{n} \sin\left(\frac{n\pi x}{L}\right)[G_n \sin(\omega_n t) + H_n \cos(\omega_n t)] \quad (8)$$

Arbitrary constants G_n and H_n are determined from the given initial conditions.

3.1.2 Forced Response: Transverse Vibration

Substituting $f(x,t) = f_0 sin(\omega t)$ in equation (6) and for a simply supported bar with boundary conditions as $w(0,t) = 0; w"(0,t) = 0$ and $w(L,t) = 0; w"(L,t) = 0$, the steady-state response of the beam undergoing transverse vibration is given by [16]

$$w(x,t) = \frac{f_0}{2\omega^2 \rho A}[\tan(\frac{\beta L}{2})\sin(\beta x) - \tanh(\frac{\beta L}{2}) \sinh(\beta x) + \cos(\beta x)\cosh(\beta x) - 2]\sin(\omega t) \quad (9)$$

4. Modal Analysis

A rectangular bar was used for the modal analysis. The length of the bar was kept constant and selected as such because the trash racks can be stacked horizontally/vertically, and its multiple lengths (1000 mm) can be used to cover the required opening considering stability, transportation, installation and maintenance. The standard thickness was chosen. Based on the thicknesses the width was chosen as per IS 11388. The bar specification and nomenclature are listed in Table 1 and Table 2 respectively.

Table 1: Bar Specification

SN	Description	Value
1	Material	Structural Steel
2	Yield Stress (YS)	250 MPa
3	Ultimate tensile strength (UTS)	410 MPa
4	Density of bar (ρ)	7850 kg/m^3
5	Young's Modulus of Elasticity (E)	200 GPa
6	Bar Spacing's (s)	30 mm, 50 mm, 80 mm, and 100 mm
7	Head Difference (H)	1 m, 2 m, 3 m, 4 m, 5 m, and 6 m

Table 2: Bar Nomenclature

SN	Dimensions (l x b x h) mm	Notation
1	1000 x 100 x 10	Bar 1
2	1000 x 120 x 12	Bar 2
3	1000 x 140 x 14	Bar 3
4	1000 x 160 x 16	Bar 4
5	1000 x 180 x 18	Bar 5

The 3D geometry of Bar 1 was created using ANSYS Design Modeler as shown in Figure 2. The Mechanical APDL solver was used for the modal analysis of the bars. The mesh was generated with an element size of 10 mm as shown in Figure 3. A simply supported boundary condition was applied in which the lower edge of one end is fixed and the lower edge of another end is allowed to move along the x-axis and restricted in the y-axis and z-axis to the geometry as shown in Figure 4. The process was repeated for Bar 2, Bar 3, Bar 4 and Bar 5.

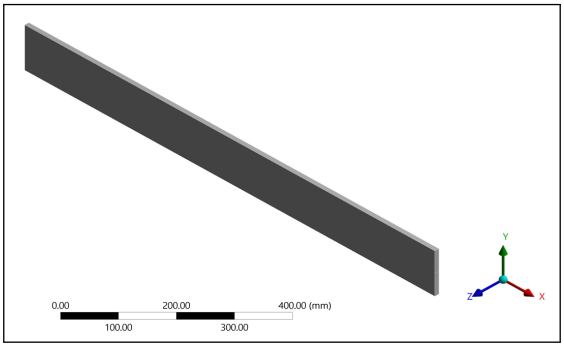

Figure 2: Bar 1: 3D Geometry

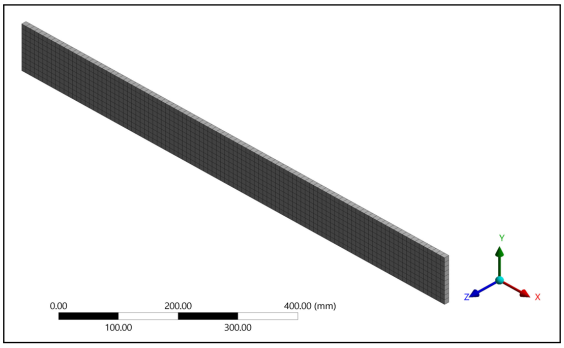

Figure 3: Bar 1: Meshing

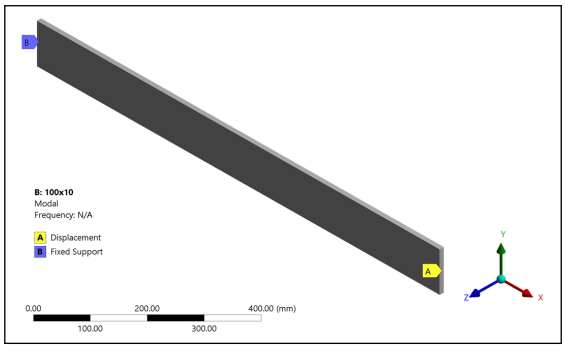

Figure 4: Bar 1: Simply Supported Boundary Conditions

The geometry, mesh and boundary conditions were completed and thirty modes were extracted. To verify the accuracy of the result, the participation factor summary was studied. The participation factor summary showed the ratio of effective mass to total mass of 0.99777 along the Y axis (transverse direction). The value close to 1 means that the significant modes have been extracted. The first three modes of transverse vibration obtained using ANSYS are shown in Figure 5, Figure 6 and Figure 7.

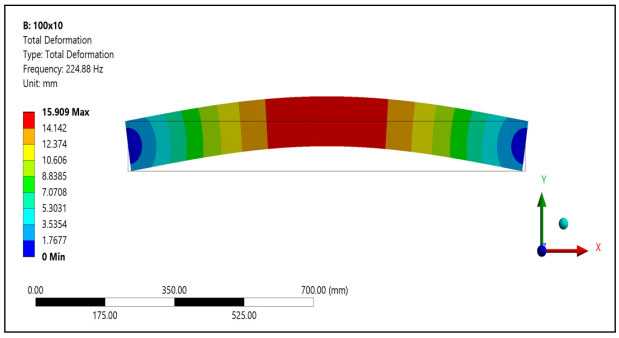

Figure 5: Mode 1: Transverse Vibration Bar 1

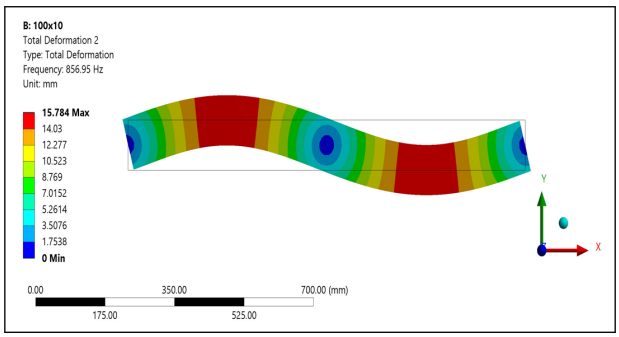

Figure 6: Mode 2: Transverse Vibration of Bar 1

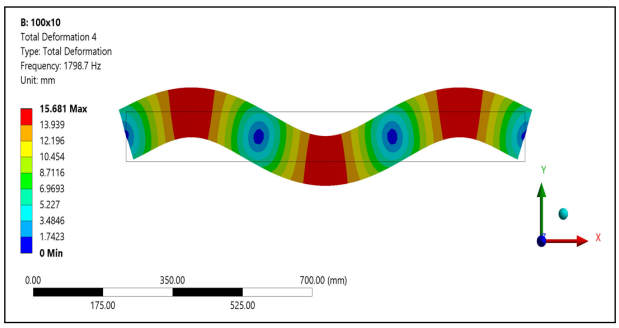

Figure 7: Mode 3: Transverse Vibration Bar 1

The analytical result of various bars with different cross-sections for the first three modes is listed in Table 3 based on Equation 7.

Table 3: Natural Frequency of First Three Modes in Hz: Analytical

SN	Notation	Mode 1	Mode 2	Mode 3
1	Bar 1	228.88	915.52	2059.93
2	Bar 2	274.66	1098.63	2471.91
3	Bar 3	320.43	1281.73	2883.90
4	Bar 4	366.21	1464.84	3295.88
5	Bar 5	411.99	1647.94	3707.87

The numerical result of various bars with different cross-sections for the first three modes is listed in Table 4 via ANSYS.

The percentage deviation between analytical and numerical results for the first three modes is listed in Table 5.

Table 4: Natural Frequency of First Three Modes in Hz: ANSYS

SN	Notation	Mode 1	Mode 2	Mode 3
1	Bar 1	224.88	856.95	1798.70
2	Bar 2	267.30	979.13	2044.50
3	Bar 3	307.66	1150.40	2239.20
4	Bar 4	345.43	1256.10	2381.20
5	Bar 5	380.17	1344.30	2472.20

Table 5: Natural Frequency of First Three Modes in Hz: Analytical vs ANSYS

SN	Notation	Mode 1	Mode 2	Mode 3
1	Bar 1	1.70%	6.40%	12.70%
2	Bar 2	2.70%	10.90%	17.30%
3	Bar 3	4.0%	10.20%	22.40%
4	Bar 4	5.70%	14.30%	27.80%
5	Bar 5	7.0%	18.40%	33.30%

5. Harmonic Analysis

The natural frequencies obtained from modal analysis were used to carry out the harmonic analysis with the mode superposition principle (MSUP). The harmonic force was calculated from 30 mm clear spacing with differential heads ranging from 1 m to 6 m. The process was repeated for the clear spacing of 50 mm, 80 mm, and 100 mm. The calculated harmonic force is listed in Table 6.

Table 6: Harmonic Force (N) for different clear spacing and differential heads

Differential Head (m)	30 mm	50 mm	80 mm	100 mm
1	294.19	490.32	784.51	980.64
2	588.38	980.64	1569.02	1961.28
3	882.57	1470.96	2353.53	2941.91
4	1176.77	1961.28	3138.04	3922.55
5	1470.96	2451.60	3922.55	4903.19
6	1765.15	2941.91	4707.06	5883.83

The calculated vortex shedding frequency for 0.75 m/s, 1.5 m/s and 3.0 m/s is listed in table 7. The geometry, mesh and boundary conditions from the modal analysis were kept the same. However, the additional boundary condition (harmonic force) was applied at the top edge which lies at the mid-span of the bar and is shown in Figure 8.

The frequency sweep was set from 0 Hz to 3000 Hz which covers all the vortex shedding frequencies under study. After the analysis, the frequency response showed that the resonant frequency may occur in the periphery of the first modal frequency and nowhere near the forcing frequencies. The bars under study were found safe. However, variables such as operating conditions under different loads, and obstruction in trash rack bars might play a vital role in attaining resonance. Therefore, considering the worst-case scenario, the resonant frequency and phase angle were noted and maximum equivalent stress was studied.

Table 7: Forcing Frequency for different Velocities in Hz

SN	Notation	**0.75** m/s	**1.5** m/s	**3.0** m/s
1	Bar 1	11.625	23.25	46.50
2	Bar 2	9.688	19.375	38.75
3	Bar 3	8.304	16.607	33.214
4	Bar 4	7.266	14.531	29.063
5	Bar 5	6.458	12.917	25.833

The failure stress and safety stress for Bars are listed in table 8 [4].

Table 8: Failure and Safe Stress in MPa

SN	Notation	Failure Stress	Safe Stress
1	Bar 1	173.625	114.593
2	Bar 2	195.938	129.319
3	Bar 3	211.875	139.838
4	Bar 4	223.828	147.727
5	Bar 5	233.125	153.863

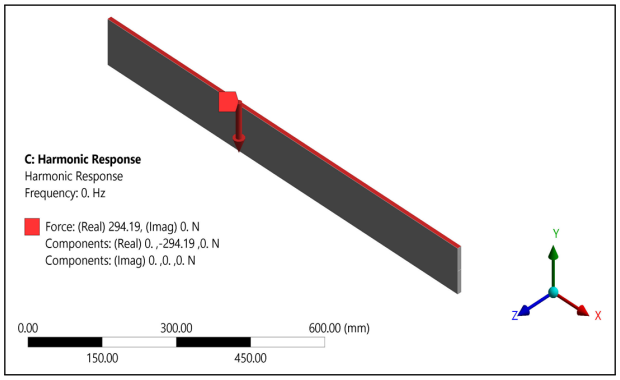

Figure 8: Bar 1: Boundary Conditions

The harmonic response analysis of Bar 1 showed that in the first mode of transverse vibration, the resonance of Bar 1 may occur at 224.79 Hz with a phase angle of 91.13°. The allowable deflection and failure stress of Bar 1 were 2 mm and 173.625 MPa respectively.

Figure 9 and Figure 10 show that Bar 1 was safe for the clear spacing of 30 mm up to 3 m, 50 mm and 80 mm up to 1 m of the differential heads. Bar 1 failed at 100 mm clear spacing at all differential heads.

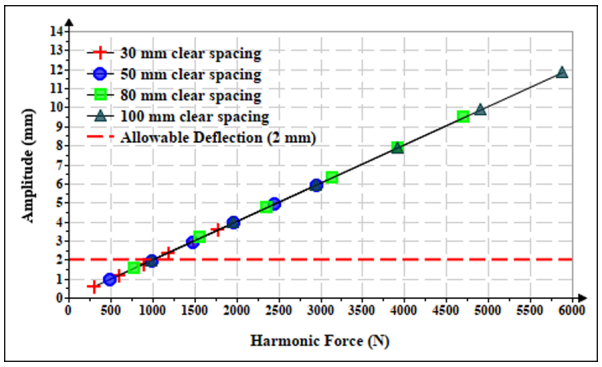

Figure 9: Bar 1: Peak Amplitude due to Harmonic Force in First Mode

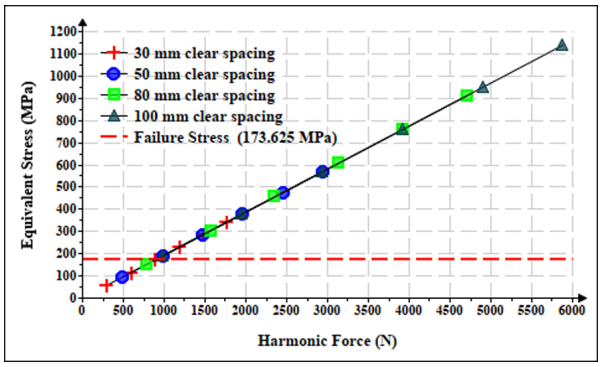

Figure 10: Bar 1: Maximum Equivalent Stress due to Harmonic Force in First Mode

The harmonic response analysis of Bar 2 showed that in the first mode of transverse vibration, the resonance of Bar 2 may occur at 267.20 Hz with a phase angle of 91.13°. The allowable deflection and failure stress of Bar 2 were 2 mm and 195.938 MPa respectively.

Figure 11 and Figure 12 show that Bar 2 was safe for the clear spacing of 30 mm up to 5 m of the differential head, the clear spacing of 50 mm up to 3 m differential head, and the clear spacing of 80 mm up to 2 m differential head and 100 mm with 1 m differential head.

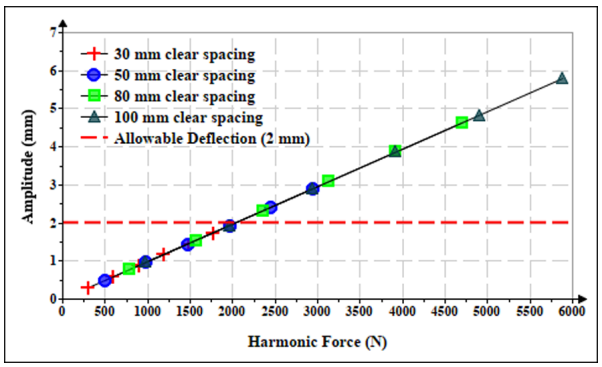

Figure 11: Bar 2: Peak Amplitude due to Harmonic Force in First Mode

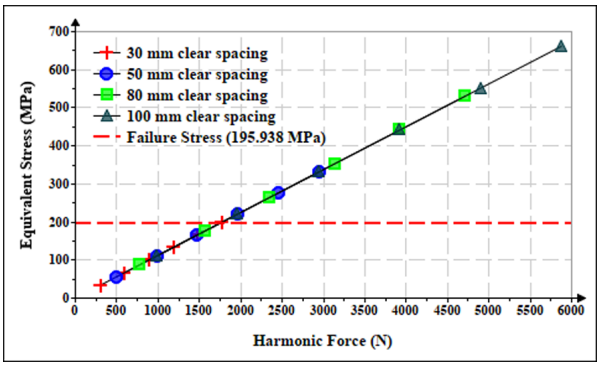

Figure 12: Bar 2: Maximum Equivalent Stress due to Harmonic Force in First Mode

The harmonic response analysis of Bar 3 showed that in the first mode of transverse vibration, the resonance in Bar 3 may occur at 307.53 Hz with a phase angle of 91.13°. The allowable deflection and failure stress of Bar 3 were 2 mm and 211.875 MPa respectively.

Figure 13 and Figure 14 show that Bar 3 was safe for the clear spacings of 30 mm and 50 mm up to 6 m of the differential head, and the clear spacing of 80 mm and 100 mm up to 3 m differential heads.

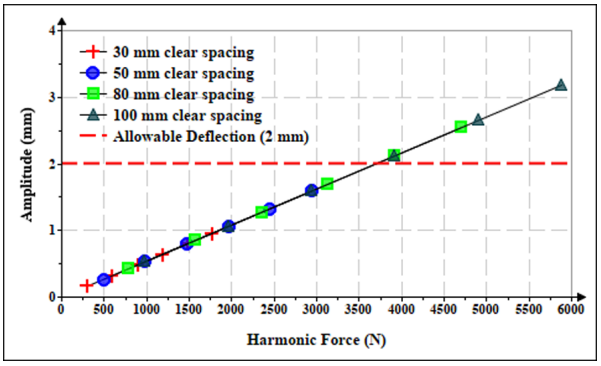

Figure 13: Bar 3: Peak Amplitude due to Harmonic Force in First Mode

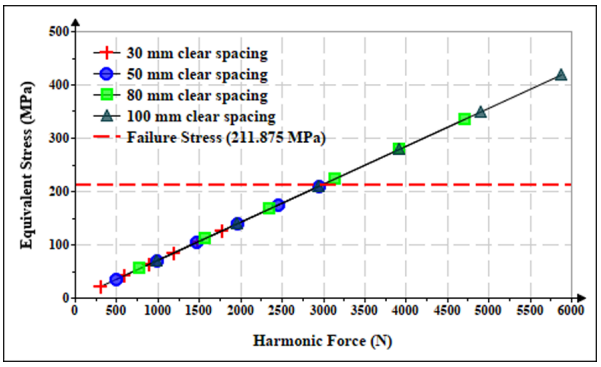

Figure 14: Bar 3: Maximum Equivalent Stress due to Harmonic Force in First Mode

The harmonic response analysis of Bar 4 showed that in the first mode of transverse vibration, the resonance in Bar 4 occurred at 345.30 Hz with a phase angle of 91.14 °. The allowable deflection and failure stress of Bar 4 were 2 mm and 223.828 MPa respectively.

Figure 15 and Figure 16 show that Bar 4 was safe for the clear spacing of 30 mm and 50 mm up to 6 m of the differential head, the clear spacing of 80 mm up to 4 m differential head and the clear spacing of 100 mm up to 3 m differential head.

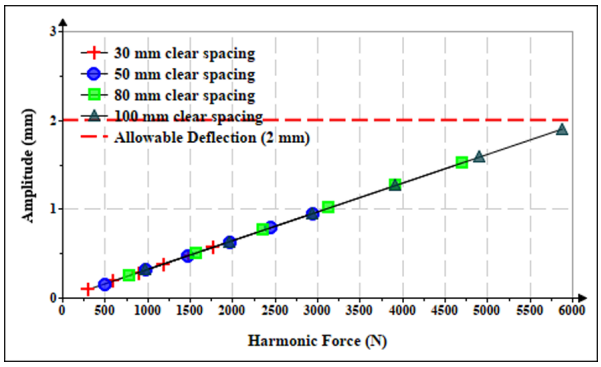

Figure 15: Bar 4: Peak Amplitude due to Harmonic Force in First Mode

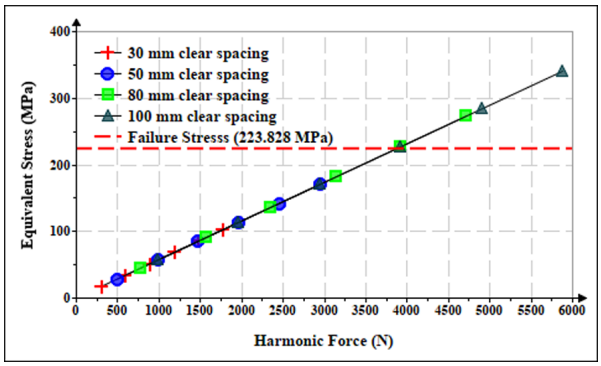

Figure 16: Bar 4: Maximum Equivalent Stress due to Harmonic Force in First Mode

The harmonic response analysis of Bar 5 showed that in the first mode of transverse vibration, the resonance in Bar 5 occurred at 380.02 Hz with a phase angle of 91.14 °. The allowable deflection and failure stress of Bar 5 were 2 mm and 233.125 MPa respectively.

Figure 17 and Figure 18 show that Bar 5 was safe for the clear spacing of 30 mm and 50 mm up to 6 m of the differential head, the clear spacing of 80 mm up to 5 m differential head, and the clear spacing of 100 mm up to 4 m differential head.

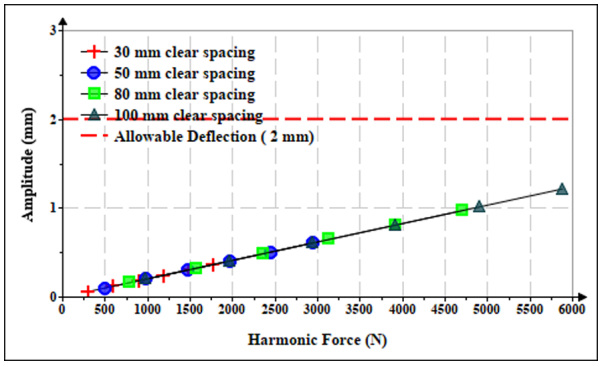

Figure 17: Bar 5: Peak Amplitude due to Harmonic Force in First Mode

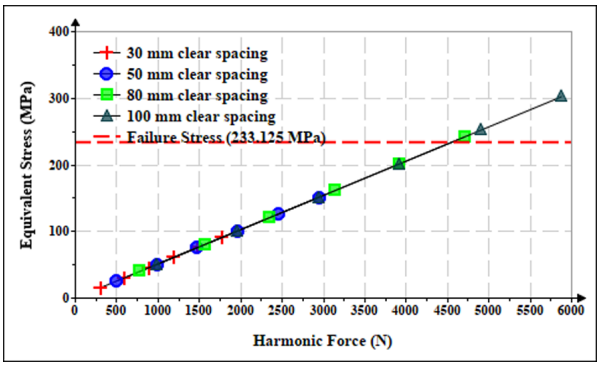

Figure 18: Bar 5: Maximum Equivalent Stress due to Harmonic Force in First Mode

6. Conclusion

In summary, the harmonic analysis of various bars with different cross-sections, clear spacing, and harmonic forces subjected to the simply supported model have been studied. The modal analysis showed the first mode of transverse vibration matches closely with the analytical result. Furthermore, the forcing frequencies being well below the natural frequencies might not cause the resonance but given the wide range of operating loads and obstruction in trash racks might. Finally, the study clearly showed that there is an almost linear relationship between harmonic force with amplitude and equivalent stress. The findings of this study can be applied during the preliminary design of trash racks related to vibration in terms of resonance, amplitude and equivalent stress. The future works could be an extended version where the whole trash rack system with water, the effect of damping and others can be incorporated.

Acknowledgments

The authors acknowledge the Department of Automobile and Mechanical Engineering, Thapathali Campus for their support, insight and encouragement.

References

[1] Leon Levin. Problèmes de perte de charge et de stabilité des grilles de prise d'eau. *La Houille Blanche*, (3):271–278, 1967.

[2] Lloyd E Sell. Hydroelectric power plant trashrack design. *Journal of the Power Division*, 97(1):115–121, 1971.

[3] Eduard Naudascher. *Flow-induced vibrations: an engineering guide: IAHR hydraulic structures design manuals 7*. Routledge, 2017.

[4] Bureau of Indian Standards. *Recommendations for design of trash racks for intakes, second revision*. Bureau of Indian Standards, 2012.

[5] LP Nascimento, JBC Silva, and V Di Giunta. Damage of hydroelectric power plant trash-racks due to fluid-dynamic exciting frequencies. *Latin American Journal of Solids and Structures*, pages 223–243, 2006.

[6] SH Crandall, S Vigander, and PA March. Destructive vibration of trashracks due to fluid-structure interaction. 1975.

[7] Thang D Nguyen and Eduard Naudascher. Vibration of beams and trashracks in parallel and inclined flows. *Journal of Hydraulic Engineering*, 117(8):1056–1076, 1991.

[8] R Hollenstein. Flow-induced vibrations of a trashrack. In *18 IAHR-congress Graz*, 1999.

[9] Xingxing Huang, Carme Valero, Eduard Egusquiza, Alexandre Presas, and Alfredo Guardo. Numerical and experimental analysis of the dynamic response of large submerged trash-racks. *Computers & Fluids*, 71:54–64, 2013.

[10] MR Haddara and S Cao. A study of the dynamic response of submerged rectangular flat plates. *Marine Structures*, 9(10):913–933, 1996.

[11] Ivan Stenius, Linus Fagerberg, and Andreas Säther. Predicting the natural frequency of submerged structures using coupled solid-acoustic finite element simulations. *Ocean Engineering*, 159:37–46, 2018.

[12] AL Gawali and CKumawat Sanjay. Vibration analysis of beams. *World Research Journal of Civil Engineering*, 1(1):15–29, 2011.

[13] Pankaj Kumar, Tejas Vispute, Anurag Sawant, Rohit Jagtap, and Girish Dalvi. Modal analysis of beam type structures. *International Journal of Engineering Research and Technololgy*, 4(4):650–654, 2015.

[14] Vaibhav Ghodge, AP Bhattu, and SB Patil. Vibration analysis of beams. *International Journal of Engineering Trends and Technology (IJETT)*, 55(2):81–86, 2018.

[15] Bing Xue, Yanpian Mao, Chunhui Zhang, Hailong Zhang, and Zhiyong Qi. Nonlinear fluid-induced vibro-impact analysis on the fatigue failure pattern of a large-scale trashrack with a reduced-order model. In *Structures*, volume 49, pages 467–478. Elsevier, 2023.

[16] Mahesh Chandra Luintel. *Textbook of Mechanical Vibrations*. Springer Nature, 2023.